INTERNATIONAL JOURNAL OF CLIMATOLOGY
Int. J. Climatol. (2009)
Published online in Wiley InterScience
(www.interscience.wiley.com) DOI: 10.1002/joc.2064

RMetS
Royal Meteorological Society

A multi-year study of sea breezes in a Mediterranean coastal site: Alicante (Spain)

Cesar Azorin-Molina,[a,b]* Deliang Chen,[c] Sander Tijm[d] and Marina Baldi[e]

[a] *The CEAM Foundation (Fundación Centro de Estudios Ambientales del Mediterráneo), Parque Tecnológico, Charles R. Darwin 14, 46980-Paterna (Valencia), Spain*

[b] *Group of Climatology, University of Barcelona, Montalegre 6, 08001-Barcelona, Catalonia, Spain*

[c] *Regional Climate Group, Department of Earth Sciences, University of Gothenburg, 40530 Gothenburg, Sweden*

[d] *Royal Netherlands Meteorological Institute (KNMI), Postbus 201, 3730-AE De Bilt, The Netherlands*

[e] *Institute of Biometeorology of the National Research Council (CNR), Via Taurini 19, 00185 Rome, Italy*

ABSTRACT: Using 6-year data collected in a high-resolution network of 19 stations in the province of Alicante (Spain), the characteristics of sea breezes for the period 2000–2005 were studied. This study attempts to develop a multi-year climatology of sea breeze flows focusing on a Western Mediterranean coastal site. We used half-hourly meteorological records from a reference station in Alicante and sea surface temperature measurements at Albufereta beach to identify past sea breeze episodes, on the basis of an objective selection technique. A total of 475 sea breeze events during the 6-year period were identified and the following parameters were determined: mean time of onset, mean wind speed and direction at the time of onset, mean time of cessation, mean temporal dimension (duration), mean maximum velocity, mean time of maximum velocity and mean wind path of the sea breeze. The mean onset and cessation times are 0940 UTC and 2009 UTC (local standard time= UTC +0100 h, or +0200 h with daylight-saving time), respectively, with a mean duration of 1029 h. The mean wind speed at the time of the passage of sea breeze fronts is low (2.07 m s^{-1}), but sea breeze gust intensities range from 3.6 to 11.6 m s^{-1} and they generally occur during 1200–1300 UTC. Southerly and southeasterly onset flows dominate in winter, whereas more easterly onsets occur in spring and summer. The mean inland directed wind path of the sea breezes is 97.7 km with noteworthy differences throughout the year; a case study showed onshore wind peaks of 11.1 m s^{-1}, 50-km inland of the Vinalopó river valley in the late afternoon. The spatial and temporal change in wind speed and direction were also analysed, using multi-year wind hodographs for the 19 stations and eight well-defined synoptic patterns favouring the development of sea breezes. Copyright © 2009 Royal Meteorological Society

KEY WORDS sea breeze parameters; wind hodographs; synoptic patterns; multi-year study; Alicante

Received 7 August 2008; Revised 13 November 2009; Accepted 14 November 2009

1. Introduction

In this paper, we study the characteristics of the sea breeze flow in the Bay of Alicante, located in southeast Iberian Peninsula (IP), in Spain. The study area is located in the Western Mediterranean basin between 37°51′N and 40°48′N, and 1°32′W and 0°31′E. The topography is quite complex due to the presence of wide and flat coastal plains on the central and south coasts, with coastal mountain ranges from the central to the northern shoreline. The river valleys are oriented approximately NNW to SSE (Vinalopó, Monnegre and Guadalest rivers, among other minor valleys), which favour the inland penetration of sea breezes. The steep Prebetic mountain ranges (1000–1600 m; Aitana is the highest mountain peak, at 1558 m) in the northern part of the province have a SW to NE orientation. The curvature of the coastline is mainly concave (Gulf of Alicante), which means the sea breeze flow should diverge in the region. However, local convex (Capes of San Antonio and Nao) and concave (Bay of Alicante) land–water boundaries are both present within the study area (Figure 1). The complex terrain have a strong influence on sea breeze circulation patterns (Johnson and O'Brien, 1973) and cause the deviation of the sea breeze flow from the ideal case (Frenzel, 1962).

The knowledge of sea breeze characteristics is usually of great interest to the vicinity of large cities (Redaño *et al.*, 1991). Alicante (5816.5 km^2) is Spain's fourth biggest province in terms of population (1 891 477 inhabitants) and population density (325.19 inhabitants km^{-2}). The coastal fringe, *Costa Blanca*, is also an area with high population density as a result of the rapid growth of tourism in the last 50 years. Thus, the study of sea breezes is important due to the impact of this flow on tourism, sports (i.e. 32nd American Cups 2007 in Valencia; Tall Ships Race 2007 and Volvo Ocean Race 2008/2009 in Alicante) and services, which are the main economic sectors of the region. In fact, sea breeze constitutes the atmospheric phenomenon that most determines

* Correspondence to: Cesar Azorin-Molina, Fundación Centro de Estudios Ambientales del Mediterráneo, Charles R. Darwin 14, 46980 Paterna (Valencia), Spain. E-mail: cazorin@ceam.es

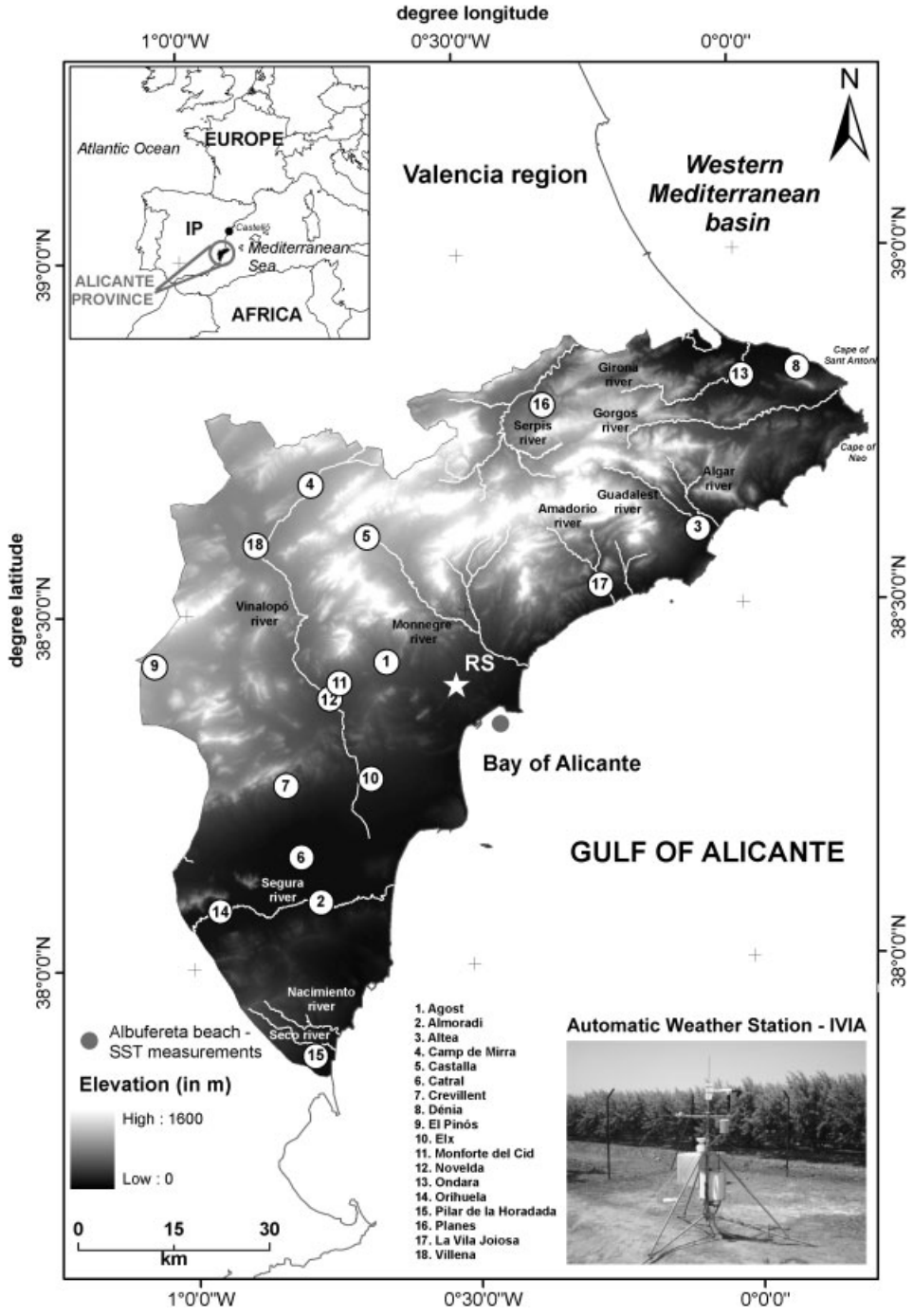

Figure 1. Terrain map of the study area showing locations of the RS, the SST measurement site (Albufereta beach) and the high-resolution network of 18 weather observation stations (numbered in Table I) used to study the dynamics of wind hodographs in the province of Alicante. Main rivers, capes and bays cited in the text are shown on the map. The inset picture corresponds to an example of the IVIA's measuring equipment (Campbell instruments).

local weather and climate, not only on the coast but also in adjacent inland areas (Simpson, 1994). Daily air temperature, humidity, wind speed and direction, precipitation and cloudiness are influenced by sea breeze circulations. This local wind constitutes the main mitigation mechanism because the intrusion of cool air associated with sea breeze circulation inhibits the increase of air temperature along the beaches and in the surrounding area. Furthermore, sea breezes enhance ventilation in air pollution episodes over coastal urban areas (Güsten *et al*., 1988; Redaño *et al*., 1991); the circulatory nature of this atmospheric circulation results in photochemical pollution (Lalas *et al*., 1983), strong vertical recirculations and a long residence time of air pollutants (Shair *et al*., 1982; Kitada *et al*., 1986), which favour chemical reactions and reduce air quality over the Western Mediterranean basin (Millán, 2002). The results presented in this study are being used in some current projects of the Air Pollutant Dynamics Area of the CEAM Foundation (www.ceam.es). For instance, the

DOI: 10.1002/joc

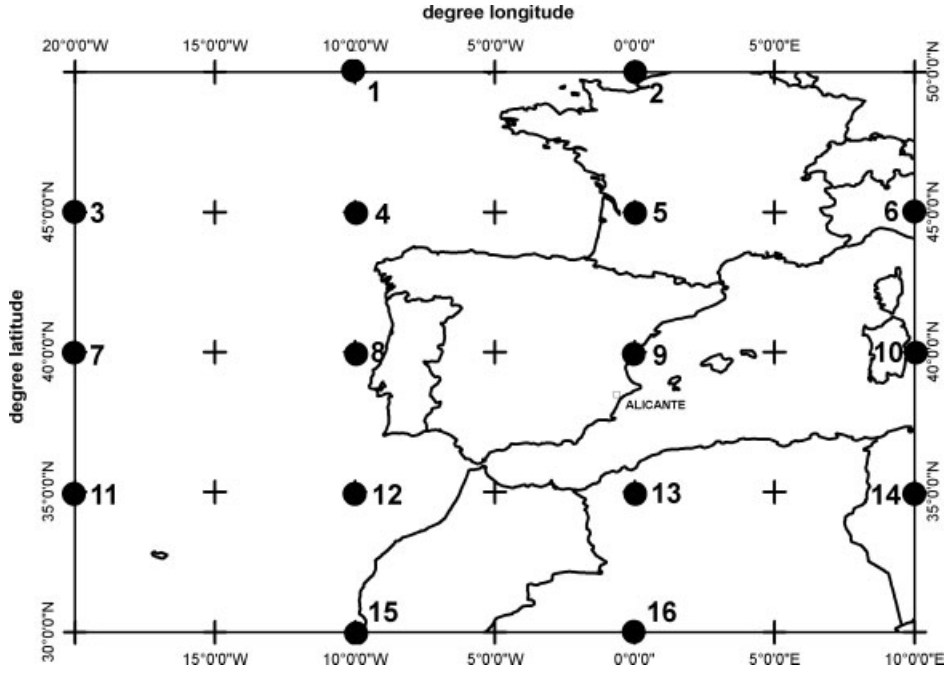

Figure 2. Location of the 16 grid points used to calculate airflow index values (see equations in Table III) and to define the large-scale circulation types associated with the development of sea breezes in the Bay of Alicante.

MECAPIP, RECAPMA and SECAP projects represent European research efforts in the study of the influence of circulatory mesoscale winds on ozone dynamics in the Mediterranean area (Millán, 2002). Consequently, there is a great need to study sea breezes.

Sea breezes constitute the major low-level mesoscale circulation during the warm season (May–October) on the Iberian Mediterranean coast, and it is due to the differential heating between land and the ocean caused by high insolation (Yan and Anthes, 1987). Although sea breezes are more frequent and persistent in spring and summer (see Chapter 4 in Azorin-Molina, 2007), they can also occur in other seasons, due to the large number of sunny days (335) throughout the year. For instance, sea breezes are often observed not only during autumn, but also during winter, when the westerly circulation is replaced by blocking anticyclones over Western Europe. A similar frequency of occurrence has been observed by Lyons (1972) for the lake breeze in Chicago.

Few studies on the sea breeze in the Bay of Alicante exist. Numerical modelling (Millán, 2002; Miao *et al*., 2003) and climatological observational (Olcina-Cantos and Azorin-Molina, 2004) techniques have been used to study the main characteristics, physical processes and effects of sea breezes on the eastern and southeastern coasts of the IP. Kottmeier *et al*. (2000) explained spatial and temporal changes in temperature, pressure, wind fields, low-level jets and strongly baroclinic zones in the southeastern of the IP (between the Mediterranean coast and some 250-km inland). On the basis of experimental data (aerological data and ground-based measurements), they concluded that these changes are due to the response of the mesoscale flow to differential heating. The study reported that low-level jets, which mark the penetration depth of sea breezes, typically penetrate to a distance of 150 km from the coast.

The main goals of this multi-year study are: (1) to determine the statistical characteristics of the major sea breeze circulation parameters in the Bay of Alicante; (2) to compute long-term half-hourly wind hodographs from a high spatial resolution surface network used for examining land–sea breeze rotation and devising statistical climatology; and (3) to identify the synoptic patterns favouring the sea breeze development. Air quality applications represent the greatest motivation for this multi-year study of the main characteristics of sea breezes.

2. Data and methods

2.1. Instrumentation and dataset

In this study, we used meteorological observations from 19 stations located both along the coast and inland in the province of Alicante (Figure 1) covering the period 2000–2005, and data on 8 March 2008 for a case study (see Section 3.5). The sites represent different topographic features that are affected by sea breezes in different ways. As a reference station (RS hereafter), we used the automatic weather station installed in the Laboratory of Climatology of the University of Alicante (38°23′N and 0°31′W; 102 m above sea level and 5.1 km from the shore; University Institute of Geography; http://www.labclima.ua.es). This site has been chosen because its location represents the general topographic characteristics of the Alicante region: a coastal plain with a concave shoreline (Bay of Alicante), with a mountain range located 10–15 km inland. The other 18 meteorological stations

DOI: 10.1002/joc

Table I. Description of the automatic meteorological stations in the province of Alicante (for locations see Figure 1).

Station	Latitude	Longitude	Height a.s.l. (m)	Dist from sea (km)	Area	Averaged days
Agost	38°25′40″N	0°38′38″W	288	16.0	P	373
Almoradí	38°05′27″N	0°46′19″W	14	11.0	P	475
Altea	38°36′21″N	0°04′40″W	84	2.5	C	475
Camp de Mirra	38°40′47″N	0°46′19″W	596	43.5	I	474
Castalla	38°36′21″N	0°40′22″W	674	31.6	I	475
Catral	38°09′17″N	0°48′14″W	5	14.9	P	475
Crevillent	38°15′25″N	0°49′44″W	199	21.0	P	474
Dénia	38°49′44″N	0°06′36″E	18	1.3	C	463
Elx	38°16′00″N	0°42′00″W	86	10.9	P	473
La Vila Joiosa	38°31′48″N	0°15′21″W	78	3.5	C	470
Monforte del Cid	38°23′59″N	0°43′44″W	277	20.8	P	455
Novelda	38°22′40″N	0°44′49″W	235	21.5	P	454
Ondara	38°49′12″N	0°00′32″E	41	5.1	C	469
Orihuela	38°02′52″N	0°57′35″W	39	24.7	P	475
Pilar de la Horadada	37°52′26″N	0°47′13″W	34	2.5	C	475
El Pinós	38°25′44″N	1°03′36″W	624	48.2	I	473
Planes	38°47′09″N	0°21′03″W	458	27.6	I	473
Villena	38°35′48″N	0°52′24″W	495	43.5	I	405
RS	38°22′99″N	0°30′67″W	102	5.1	C	475

Coast (C), inland (I) and prelittoral (P) locations. Last column corresponds to the number of averaged days for computing the wind hodographs.

belong to a high spatial resolution surface network maintained by the Valencian Institute for Agriculture Research (IVIA, http://www.ivia.es/estacion/; Ministry of Agriculture, Food and Fisheries, Valencia Regional Government). Half-hourly average observations (with a sampling time of 10 s) of horizontal wind speed (WS, in m s^{-1}), wind direction (WD, in degree and stored in 1° steps), air temperature (TEMP, in°C), relative humidity (RH, in %) and other meteorological variables have been continuously recorded at each station since 2000. The WS is recorded at a height of 2 m, and therefore we used the formula given in Justus and Mikhail (1976) to obtain the horizontal WS at 10 m:

$$\mathrm{WS}(Z) = \mathrm{WS}(R) \times \left(\frac{Z}{Z_r}\right)^N \qquad (1)$$

where WS(R) is the WS at a height of 2 m, Z and Z_r are the height of 10 and 2 m, respectively, and N is an empirical constant that depends on the speed at the reference height (Reed, 1974), the atmospheric stability (Smith, 1968), and the surface roughness (Davenport, 1963). TEMP and RH were measured at 1.5 m above the surface. All the data have been quality controlled (QC) by applying the tests referred in the literature (Graybeal *et al*., 2006) to detect any unrealistic value (out-of-range records). Meteorological variables at the RS have been measured at 10 m above the surface and used to create the climatology of sea breezes in the Bay of Alicante. We then analysed data from the 18 IVIA stations focussing on the rotation of the wind shown by hodographs. A detailed description and location of the measuring equipment used here is given in Figure 1 and Table I.

Monthly sea surface temperature (SST), provided by the Institute of Coastal Ecology of El Campello (Alicante; http://www.ecologialitoral.com/), was measured 0.27 nautical miles (i.e. 0.5 km) offshore and at a depth of 4–5 m on the Albufereta beach (38°21′N and 0°26′W), which is exactly adjacent to the RS (6.3 km). Daily SST was obtained by linearly interpolating the monthly data. This is the most consistent and reliable SST dataset in the province of Alicante, given that 1-h TEMP data from the nearest buoy has been available since July 2006 (Cape of Palos buoy; 37°39′N, 0°19′W http://www.puertos.es/en/oceanografia_y_meteorologia/redes_de_medida/index.html). In a similar study of sea breeze in Sardinia (Italy), Furberg *et al*. (2002) used monthly averaged SST in lieu of daily values.

2.2. Sea breeze detection

In order to detect sea breeze episodes, we used an automated selection technique based on two filter groups: (1) distinctive features in WS and WD, as the characteristic rapid shift in WS and WD at onset and cessation time, as well as the maximum WS ($\mathrm{WS_{max}}$) of sea breezes (Borne *et al*., 1998) and (2) physical processes of sea breezes as the semi-diurnal pressure wave or diurnal air pressure amplitude (Prtenjak and Grisogono, 2007) in combination with a positive difference in temperature between the daily maximum TEMP at the RS and the SST ($\Delta T > 0$ °C, Laird *et al*., 2001). A subset of 475 episodes met the sea breeze requirements at the RS during the period 2000–2005, with sea breeze episodes occurring in presence of weak large-scale flows. Table II displays a summary of the monthly probability [$p_1 = (1)/N$] of sea breeze episodes identified by the automated selection methodology for the 6-year study period.

DOI: 10.1002/joc

Table II. Probability (p_1) of sea breeze days detected by the automated selection methodology for the 6-year study period (2000–2005).

	J	F	M	A	M	J	J	A	S	O	N	D
2000	0.10	0.00	0.10	0.07	0.45	0.50	0.65	0.10	0.10	0.06	0.00	0.03
2001	0.00	0.11	0.03	0.20	0.29	0.43	0.39	0.48	0.00	0.26	0.03	0.10
2002	0.29	0.29	0.13	0.23	0.23	0.47	0.39	0.45	0.17	0.16	0.07	0.06
2003	0.06	0.11	0.26	0.23	0.35	0.40	0.52	0.52	0.10	0.10	0.03	0.06
2004	0.26	0.17	0.06	0.20	0.26	0.60	0.45	0.45	0.23	0.19	0.20	0.00
2005	0.29	0.07	0.10	0.30	0.26	0.43	0.29	0.16	0.27	0.13	0.03	0.00
Mean	0.17	0.12	0.11	0.21	0.31	0.47	0.45	0.36	0.14	0.15	0.06	0.04

The local geometry of the coastline (62°–242°) adjacent to the RS was considered and the sea and land breeze central axes are therefore 152° and 332°, respectively. Observational campaigns detected that the local geometry and topography of the coastline cause certain changes in the direction of land–sea breezes. Consequently, sea breezes blow from 45° to 180° (clockwise) and the Coriolis force can produce sea breezes from 180° to 225° in the late evening, that is, almost parallel to the coastline. Sea breezes at RS present the following characteristics:

1. *Onset*: Onset is defined as the sea breeze passage between 0100 and 0730 hours after local sunrise (LSR). The onset is defined as the time when the 30-min mean WS (WS_x) is equal to or higher than 1.5 m s^{-1} and the 30-min mean WD (WD_x) is simultaneously between 45° and 180° (clockwise rotation). Previous WS_x and WD_x must be less than 1.5 m s^{-1} or between 181° and 44° (land breeze; clockwise rotation), respectively. In the present study, we analysed onset time (O_{time}), onset speed (O_{ws}) and onset direction (O_{wd}). Times in this study are given in UTC: local time in Alicante is UTC +0100 h, or +0200 h with daylight-saving time.
2. *Cessation*: Cessation is defined as the time when the sea breeze front withdraws between 1 h before and 5 h after local sunset (LSS). Cessation time (C_{time}) is when the 30-min maximum WS (WS_{max}) is less than 1.5 m s^{-1} or WD_x is between 226° and 44° (land breeze; clockwise rotation). At the end of the sea breeze period, this local wind can blow parallel to the coastline (between 181° and 225°, clockwise rotation) due to the Coriolis force and topography.
3. *Duration (D_t)*: Period of time between the O_{time} and C_{time} of the sea breeze.
4. *Maximum velocity (WS_{max}) and WS_{max}* time: WS_{max} is the maximum WS reached during the sea breeze occurence.
5. *Sea breeze wind path (SB_{path})*: The horizontal extent of the sea breeze from the coastline was calculated as follows (Salvador and Millán, 2003):

$$\text{SB}_{\text{path}} = \sum \sqrt{u^2 + v^2} \times \Delta t \qquad (2)$$

where u and v are the westeast and northsouth components (Stull, 1995) of the sea breezes and Δt is equal to the sampling time of the wind data, that is, 30 min. This formula gives the distance that a particle travels if the vector wind is constant along its displacement, and it provides a preliminary estimation of the inland directed wind path of the sea breeze using a single observation point and without considering density across the front (Physick, 1980), soil characteristics or topography, which can have strong local effects (Simpson, 1994). An understanding of the inland directed wind path of the sea breeze is of great interest, particularly for air quality applications, as pointed out Azorin-Molina *et al.* (2008).

2.3. Synoptic weather types: Jenkinson and Collison method

Figure 2 represents the domain where Vicente-Serrano (2004) applied the automated circulation typing scheme of Jenkinson and Collison (1977) (hereafter JC method) to the IP. The JC method is the automated version of the Lamb scheme (Lamb, 1950), which is the best-known manual scheme for the British Isles (Jones *et al.*, 1993). The JC method can be applied in any mid-latitude zone (e.g. Chen, 2000). Sea level pressure (SLP) in the domain is given at 16 grid points every 5° in latitude and 10° in longitude (Jones *et al.*, 1993; Linderson, 2001). The daily SLP values [$p(n)$] are extracted from the National Centre for Environmental Prediction (NCEP) and the National Centre for Atmospheric Research (NCAR) reanalysis project (http://www.cdc.noaa.gov/cdc/reanalysis/reanalysis.shtml; Kalnay *et al.*, 1996) for the 6-year study period (2000–2005).

The JC method is based on objective rules that are used to calculate seven circulation indices, as summarized in Table III. Using these objective rules, we calculate the geostrophic wind (Wg) and vorticity to determine Lamb's weather type defined for the British Isles. Equation (1) in Table III gives the surface westerly component (u) of the Wg calculated from the surface pressure gradient between 12–13 (35.0 °N) and 4–5 (45.0 °N) grid points; Equation (2) gives the surface southerly component (v) of the Wg computed from the surface pressure gradient between 5–9–13 (0.0°) and 4–8–12 (10.0 °W) grid points; Equation (3) gives the surface Wg; Equation (4) gives the WD in degree (from 0° to 360°), calculated as follows: if $u > 0$ and $v < 0 = 360 + D$ (4° quadrant); if $u > 0$ and $v > 0 = 180 + D$ (3° quadrant); if $u < 0$ and $v > 0 = 180 + D$ (2° quadrant) and if $u < 0$ and

DOI: 10.1002/joc

Table III. Equations adapted from Jenkinson's and Collison's objective method (1977).

$$u = 0.5(p12 + p13) - 0.5(p4 + p5) \quad (3)$$
$$v = 1.74[0.25(p5 + 2p9 + p13) - 0.25(p4 + 2p8 + p12)] \quad (4)$$
$$V = (u^2 + v^2)^{1/2} \quad (5)$$
$$\mathrm{Dir} = \tan^{-1}(u/v) \quad (6)$$
$$\xi_u = 1.07[0.5(p15 + p16) - 0.5(p8 + p9)] - 0.95[0.5(p8 + p9) - 0.5(p1 + p2)] \quad (7)$$
$$\xi_v = 1.52\begin{bmatrix} 0.25(p6 + 2p10 + p14) - 0.25(p5 + 2p9 + p13) \\ -0.25(p4 + 2p8 + p12) + 0.25(p3 + 2p7 + p11) \end{bmatrix} \quad (8)$$
$$\xi = \xi_u + \xi_v \quad (9)$$

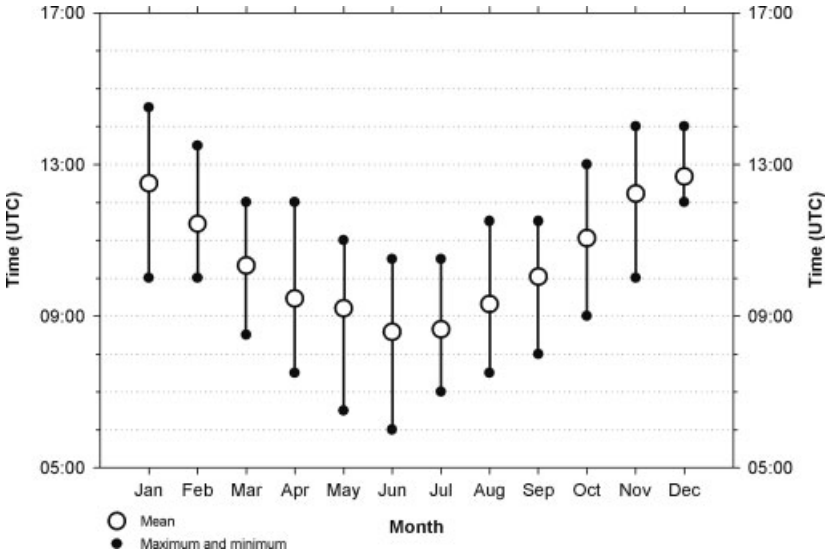

Figure 3. Monthly mean and range of sea breeze onset time (in UTC) for the 6-year study period (2000–2005).

$v < 0 =$ WD (1° quadrant); Equations (5) and (6) give, respectively, the westerly (ξ_u) and southerly (ξ_v) components; and Equation (7) gives the total vorticity (ξ). The constants used in the equations (1.74; 1.07; 0.95 and 1.52), taken from Vicente-Serrano (2004), are calculated using the methodology proposed by Dessouky and Jenkinson (1975) and derived from relative differences between grid point size in the eastwest and northsouth directions.

The synoptic catalogue identifies 27 weather types grouped into four categories: (1) directional flow types (N; NE; E; SE; S; SW; W; NW) characterized by coherent WD ($|\xi| < V$); (2) anticyclonic (A, if $|\xi| < 0$) and cyclonic (C, if $|\xi| > 0$) types related to the rotation of the atmosphere ($|\xi| > 2V$); (3) hybrid types ($V < |\xi| < 2V$), which depend on the Z and the WD (AN; ANW; AW; ASW; AS; ASE; AE; ANE; CN; CNW; CW; CSW; CS; CSE; CE; CNE) and (4) the unclassified type (UD, Jones *et al*., 1993) where $V < 6$ and $|\xi| < |6|$. The JC objective method has been successfully applied by several authors (Spellman, 2000; Martin-Vide, 2001; Vicente-Serrano, 2004) to study the relationship between climate variables and atmospheric circulation over the IP. Two main limitations have been envisaged by Spellman (2000): (1) the automated method gives almost one UD type in every five (i.e. 18.4%), preferably in summer and autumn, when weak surface pressure gradients dominate; however, the extension of the original grid basis of Spellman (2000) enabled the UD type to be classified; (2) the high frequency of the C weather type in summer, in relation to the daily thermal low forming over the IP. This is not a limitation for sea breeze studies, as this C weather type tends to enhance sea breeze development.

3. Results

3.1. Onset features of the sea breeze

3.1.1. Mean time of the sea breeze passage

The O_{time} mainly depends on latitude (Yan and Anthes, 1987), season (Novak and Colle, 2006), local topography (Ookouchi and Wakata, 1984), vegetation (Segal *et al*., 1988), soil (Miao *et al*., 2003), SST (Bowers, 2004) and atmospheric conditions (Estoque, 1962). The mean O_{time} is 0940 UTC for the 6-year study period, and it varies between 0855 and 0955 UTC. The interannual variation of the O_{time} is associated with the climate conditions for each year. The maximum relative frequency of the O_{time} for the whole study period occurs between 0830 (14.5%) and 0930 (14.5%) UTC, 0900 UTC being most frequent (15.4%). The sea breeze passage varies from 0600 UTC (1–2 hs after LSR in summer) to 1430 UTC (7–8 h after LSR in winter) throughout the year. Figure 3 presents the

DOI: 10.1002/joc

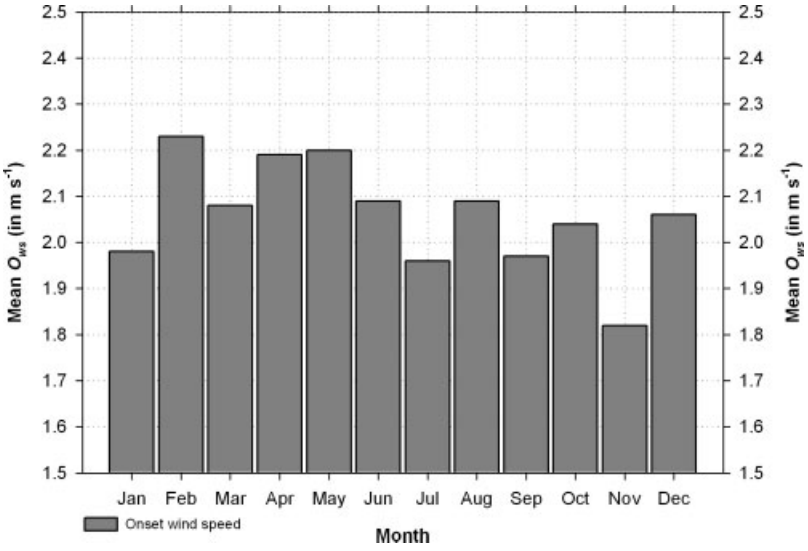

Figure 4. Mean monthly sea breeze WS at the time of onset for the 6-year study period (2000–2005).

monthly variation in O_{time}, which gradually decreases from winter to summer and slowly increases in the opposite direction from summer to winter. The earliest O_{time} occurs at 0834 UTC in June (summer solstice), whereas the latest O_{time} takes place at 1241 UTC in December (winter solstice). The monthly statistics show a clear seasonal variation of the O_{time}.

3.1.2. *Wind speed at the onset*

The WS_x at the time of onset (O_{ws}) of the sea breeze constitutes an interesting characteristic, which has not been previously studied. The O_{ws} was computed for the 475 episodes and the velocities grouped into seven points according to the eight categories of WS_x found in the RS: 1.8, 2.2, 2.7, 3.1, 3.6, 4.0 and 4.5 m s^{-1}, with a mean value of 2.07 m s^{-1} in the 6-year study period. The 1.8 m s^{-1} interval provides the highest relative frequency (56.2%). The 2.2 and 2.7 m s^{-1} intervals also display relatively high frequencies, covering 29.5% and 10.1%, respectively. Few events were observed in the intervals corresponding to the strongest sea breeze passages: 3.1 m s^{-1} (2.3%), 3.6 m s^{-1} (1.3%), 4.0 m s^{-1} (0.4%) and 4.5 m s^{-1} (0.2%). In conclusion, the mean WS of sea breeze passages at the time of onset is usually low.

Figure 4 shows the mean monthly O_{ws} for the 6-year period: April (O_{ws} 2.19 m s^{-1}) and May (O_{ws} 2.20 m s^{-1}) show high mean O_{ws} in relation to the biggest land–sea air ΔT throughout the year (Zhong and Takle, 1993; Laird *et al*., 2001). Nonetheless, an exception was detected, as February presents the strongest mean O_{ws} (2.23 m s^{-1}). This was due to the extraordinary O_{ws} observed on 22 February 2002 (4.5 m s^{-1}) and on 2 February 2005 (3.6 m s^{-1}). In contrast, a low mean O_{ws} was measured in July (1.96 m s^{-1}) because summer low-level thermal inversions associated with continental tropical air masses from Africa (see C weather type in Figure 14f) weaken the O_{ws} (Ramis *et al*., 1990). The lowest mean O_{ws} is measured in November (1.82 m s^{-1}), as we expect, due to the lower land–sea air ΔT in autumn months. The seasonal statistic of the mean O_{ws} confirms the monthly behaviour with the lowest value in autumn (S-O-N: 1.94 m s^{-1}), the highest in spring (M-A-M: 2.16 m s^{-1}), and mid values in winter (D-J-F: 2.09 m s^{-1}) and summer (J-J-A: 2.05 m s^{-1}).

3.1.3. *Wind direction of the sea breeze passage*

The bar chart in Figure 5 shows the relative frequency distribution (n_i, %) of the WD at the time of onset (O_{wd}) in the Bay of Alicante. The initiation of sea breezes can be between 45° and 180°, and WD data were grouped into seven compass points. Sea breezes preferably tend to initiate from 67.5° (19.4%), 90° (18.3%) and 112.5° (17.9%). The relative frequency distribution of O_{wd} is also high for 135° (14.5%) and 157.5° (14.7%), but it shows a limited number of occurrences of sea breezes initiating at 45° (7.8%) and 180° (7.4%).

Monthly relative frequency distribution of O_{wd} is reported in Table IV, showing a clear monthly variation with a tendency for sea breeze to initiate between 135° and 180° during autumn and winter. For instance, the highest relative frequency distributions are 29.0% and 25.8% in January for the 157.5° and 180° components, respectively. We detected an identical behaviour pattern in October (25.0% for 135°), November (36.4% for 157.5°) and December (25.0% for 157.5° and 180°, as well as for 67.5°). In contrast, the initial direction of sea breeze flow is between 67.5° and 112.5°, that is, most easterly flows, in May (28.1% for 90°), June (24.7% for 67.5°), July (24.1% for 67.5°), August (26.9% for 112.5°) and September (26.9% for 112.5°). This was also found by Salvador and Millán (2003) for the climatology of sea breezes in Castellon (east of the IP). They concluded that the O_{wd} depends on the declination of the sun (sunrise takes place between N and E in summer and between E and S in winter) and the orientation of hillsides. The southerly component of sea breezes

DOI: 10.1002/joc

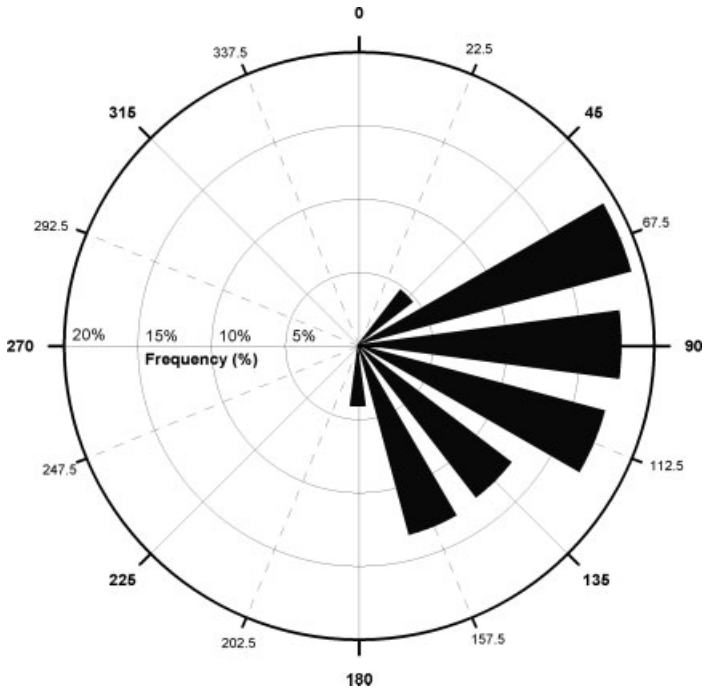

Figure 5. Polar bar chart of the relative frequency distribution of sea breeze WD (°) at the time of onset for the 6-year study period (2000–2005).

Table IV. Monthly relative frequency distribution (n_i, %) of WD at the time of onset for the 6-year study period (2000–2005).

WD (°)	J	F	M	A	M	J	J	A	S	O	N	D
45	0.0	9.5	14.3	8.1	5.3	7.1	12.0	9.0	7.7	7.1	0.0	0.0
67.5	9.7	**23.8**	9.5	**16.2**	17.5	**24.7**	**24.1**	22.4	19.2	10.7	0.0	**25.0**
90	12.9	14.3	4.8	**16.2**	**28.1**	21.2	20.5	16.4	19.2	17.9	0.0	12.5
112.5	16.1	**23.8**	**38.1**	**16.2**	14.0	12.9	14.5	**26.9**	**26.9**	10.7	18.2	0.0
135	6.5	9.5	14.3	**16.2**	14.0	15.3	15.7	10.4	15.4	**25.0**	27.3	12.5
157.5	**29.0**	14.3	14.3	**16.2**	15.8	11.8	10.8	11.9	7.7	17.9	**36.4**	**25.0**
180	25.8	4.8	4.8	10.8	5.3	7.1	2.4	3.0	3.8	10.7	18.2	**25.0**

The highest relative frequency distribution for each month is shown in bold face.

in autumn and winter is induced by daytime diabatic heating of the sloping terrain (Prebetic mountain slopes; mountain/valley breezes), which forces sea breezes to blow between 135° and 180°. This can be explained as the result of the combined effect of mountain/valley and sea breezes. The easterly direction of sea breezes in spring and summer months is associated with the thermal low pressure developed over the centre of the IP and the north of Africa (Millán *et al*., 2002; see C weather type in Figure 14f).

3.2. Mean time of sea breeze cessation

The mean cessation time of sea breezes depends on the same factors as described above for O_{time}. The mean value of C_{time} during the 6-year period is 2009 UTC, and it varies from 1947 to 2039 UTC. The maximum frequency of C_{time} occurs between 2000 UTC (12.4%) and 2100 UTC (12.8%). C_{time} varies from 1630 UTC (1 h before LSS in winter) to 2330 UTC (4–5 h after LSS in summer) throughout the year. C_{time} also shows a pronounced monthly variation in relation to the season. Figure 6 displays the monthly variation in C_{time} that gradually increases from 1729 UTC in January to 2005 UTC in April but is still slowly increasing from 2033 UTC in May to 2128 UTC in July; and a sharp decline is detected from 2107 UTC in August to 1943 UTC in September. Thus, the earliest C_{time} is at 1718 UTC in December (winter solstice) and the latest C_{time} is at 2128 UTC in July (shortly after the summer solstice).

3.3. Mean duration of sea breeze flow

The daily duration of sea breeze flows was computed from the onset and cessation time for each episode. The mean D_t is 1029 h for the 6-year period. We detected noteworthy differences, however, between the highest D_t observed in 2000, 1144 h, and the lowest D_t measured in 2005, 0953 h. The maximum D_t frequency is found between 1100 and 1300 h, the class of 1100 h being the most frequent one (8.6%). The daily duration fluctuates greatly from a minimum of 0230 h in autumn–winter to a maximum of 1600 h in summer. Figure 7 shows that the mean monthly duration of sea breezes gradually

DOI: 10.1002/joc

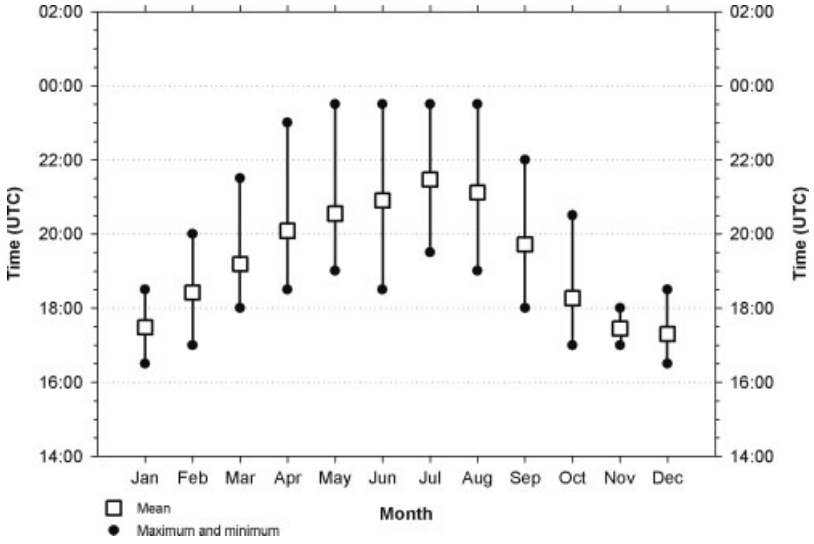

Figure 6. Monthly mean and range of sea breeze cessation time (in UTC) for the 6-year study period (2000–2005).

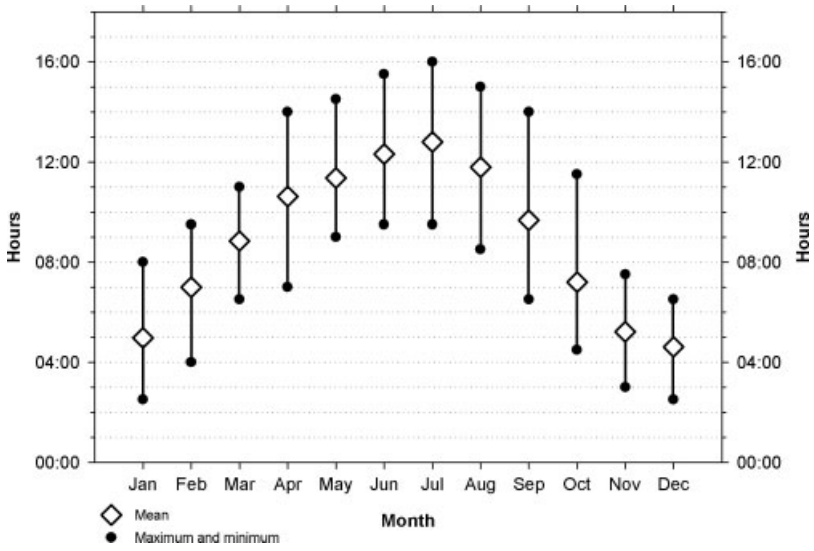

Figure 7. Monthly mean and range of sea breeze duration time for the 6-year study period (2000–2005).

increases from January (0459 h) to July (1248 h), when it reaches its highest, then it steadily decreases from the central summer months until December (0437 h), when it reaches its minimum value.

3.4. Mean maximum velocity and mean time of maximum velocity of the sea breeze

A well-developed low-level circulation occurs in the Bay of Alicante during sea breeze events. Sea breeze gust intensities range from a minimum of 3.6 m s^{-1} to a maximum of 11.6 m s^{-1}, and the mean maximum velocity (WS_{max}) is 6.8 m s^{-1} for the 6-year period. Maximum velocities greater than 10.5 m s^{-1} are rare, and only during three episodes, gusts exceeded this value: 10.7 m s^{-1} (26 May 2004), 11.2 m s^{-1} (12 May 2002) and 11.6 m s^{-1} (11 August 2004).

The 6–7 m s^{-1} class interval shows the highest relative frequency of maximum velocities: 32.4%, whereas class intervals 5–6, 7–8 and 8–9 m s^{-1} also exhibit high relative frequencies with 18.7%, 21.5% and 13.5%, respectively. On an annual scale, WS_{max} fluctuates between a maximum of 7.3 m s^{-1} for the year 2000 and a minimum of 6.5 m s^{-1} for the years 2001 and 2005: 6.7 m s^{-1} for 2002 and 6.8 m s^{-1} for 2003 and 2004. However, the summer vertical stability and the upper stable layers acted as a strong damping mechanism in many summer days in 2003. The low-level thermal inversions associated with continental tropical (cT) air masses from Africa weakened sea breezes. These results well agree with those obtained by Prtenjak and Grisogono (2007), who reported maximum velocities of sea breezes between 6 and 8 m s^{-1} for the northern Croatian Adriatic coast.

Figure 8 shows the monthly WS_{max} calculated over the 6-year study period: sea breezes are much stronger from April to August, particularly during the spring months due to the biggest land–sea air ΔT: April (7.7 m s^{-1}), May (7.4 m s^{-1}), June (7.2 m s^{-1}), July (7.0 m s^{-1}) and August (6.9 m s^{-1}). In contrast, light sea breezes occur

DOI: 10.1002/joc

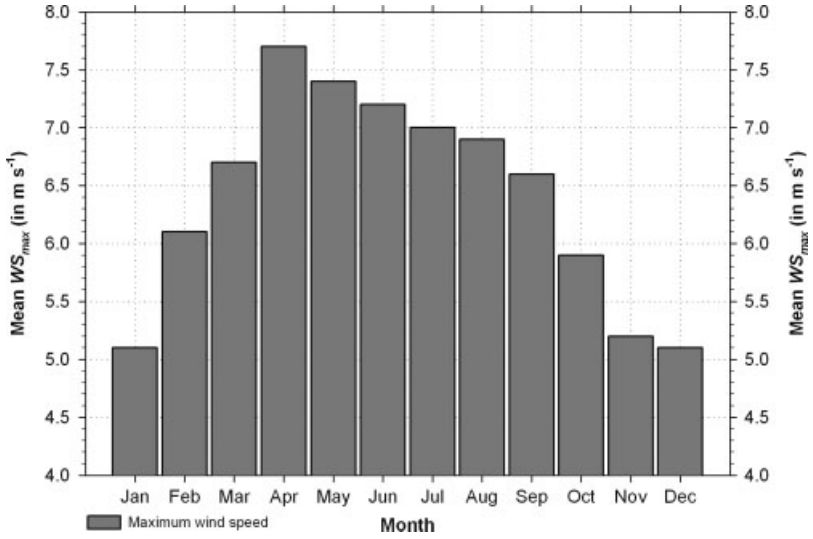

Figure 8. Mean monthly maximum WS for the 6-year study period (2000–2005).

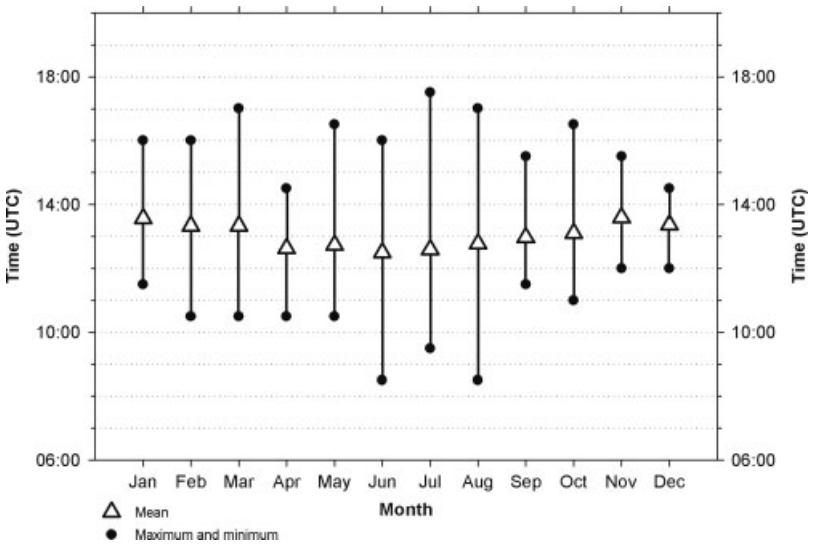

Figure 9. Monthly mean and range of the maximum velocity time (in UTC) of sea breezes for the 6-year study period (2000–2005).

from September to March when the land–sea air ΔT is smallest.

The mean time of maximum velocity (WS_{time}) during the study period is 1250 UTC. The time of maximum velocity of sea breeze occurs at 1230 UTC with a frequency of 13.5%, followed by 1300 UTC with a frequency of 13.3% and by 1200 UTC (12.4%). We measured maximum sea breeze gust velocities between 0830 and 1730 UTC. The difference in annual average with respect to WS_{time} ranges from 07′ (1257 UTC in 2003) to −15′ (1235 UTC in 2001). Finally, Figure 9 shows the mean monthly statistics of maximum sea breeze velocities, which provide valuable information on the intraannual variation in WS_{time}. The time of maximum velocity of sea breezes occurs earlier during the day relative to the mean, in the months from April to August, and later from September to March. WS_{time} is also determined by the pressure gradient that was built during the day due to the differential heating over land and over the sea. The more intense this differential heating during spring–summer months, the higher the maximum velocities of sea breezes are and the earlier they occur. For instance, WS_{time} fluctuates from as early as 1230 UTC in June to as late as 1335 UTC in November.

3.5. Mean sea breeze wind path. A case study of a strong sea breeze front

The mean SB_{path} at the reference station is 97.7 km for the 6-year study period. Maximum wind path of sea breezes were 224.7 km on the 12 July 2003 and 187.6 km and 178.9 km on the 5 July 2000 and 8 May 2001, respectively, whereas minimum wind path of sea breezes were measured on the 2 December 2001 and the 23 November 2004: 18.4 km. In a summary of some sea breeze studies, Atkinson (1981) reported maximum inland propagation of the front between 30 and 300 km.

The class interval of 100–125 km contains the highest frequency distribution of sea breeze wind paths, 33.1%,

DOI: 10.1002/joc

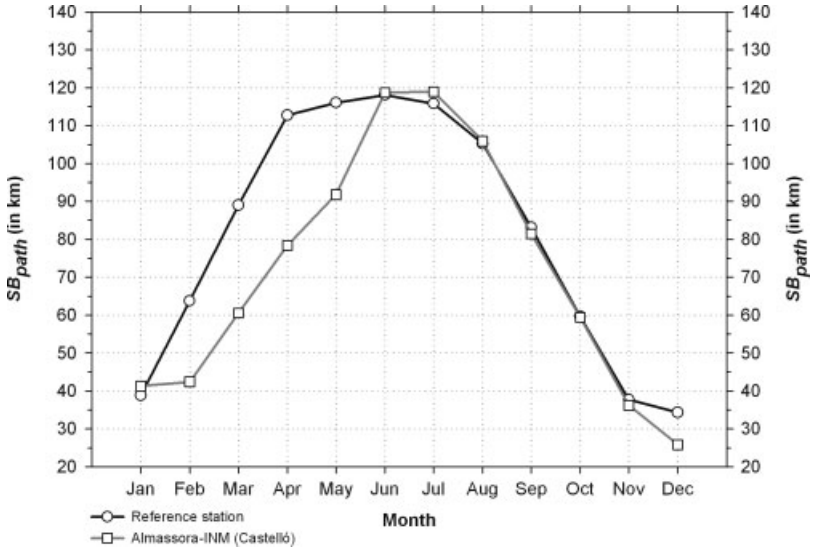

Figure 10. Mean monthly wind path (in km) of sea breezes for the 6-year study period (2000–2005) in comparison with mean monthly values calculated by Salvador and Millán (2003) in Almassora station (Castelló) for the 1983–1991 study period.

followed by the class interval of 75–100 km, which represents 23.8% of sea breeze episodes. The inland directed wind path is usually between 25 and 175 km, whereas few sea breeze wind paths above or below this value were observed. The annual mean SB_{path} is equal to 119.1 km in 2000; 98.3 km in 2001; 93.6 km in 2002; 98.5 km in 2003; 92.8 km in 2004 and 88.1 km in 2005. In addition, SB_{path} shows a marked monthly variation, with a gradual increase from 38.8 km in January to 118.1 km in June, followed by a dropping to 34.7 km in December, which represents the minimum monthly SB_{path}. Figure 10 shows a close connection between the monthly SB_{path} values for the Bay of Alicante and those computed by Salvador and Millán (2003) for Almassora station (Castelló; north of the Valencia region, Figure 1) using the same technique.

An observational case study on the spread inland of sea breezes along the Vinalopó river valley (Figure 1) is presented here. 8 March 2008 is a winter day that represents the deep inland invasion of sea breezes in the southeast of the IP. The weather was generally clear and the synoptic pressure gradient was weak. A very good indicator of the arrival of sea breezes has been obtained measuring WS, WD, TEMP and RH (Simpson, 1994) from stations located at different distances from the coastline (Figure 1): Elx (10.9 km), the Monforte del Cid (20.8 km), the Villena (43.5 km) and the Camp de Mirra (43.5 km) stations. The arrival of sea breezes was detected in each of the five experimental sites examining the characteristics changes in WS, WD, TEMP and RH displayed in Figure 11. Cool marine air propagated inland when a cross-shore mesoscale pressure gradient was created by daytime differential heating. The frontal passage of sea breezes (transition between continental air masses and marine air masses) occurred between 3 and 5 h earlier for the prelittoral stations in comparison with the inland stations: Elx (1200 UTC), Monforte del Cid (1330 UTC), Villena (1700 UTC) and Camp de Mirra (1730 UTC). Sea breezes were clearly observed in the form of a front, with sudden shifts in WS, WD, TEMP and RH. The RH rise (∼10% in the prelittoral stations against ∼20–25% in the inland stations between periods of 30-min) and TEMP decrease (∼1.5 °C against ∼3.5 °C) were even more marked in the inland stations, as reported in Simpson (1994). In addition, an abrupt rise of WS (maximum wind speeds of 11.1 m s^{-1}) was observed in the Villena station in the late afternoon. Kottmeier *et al.* (2000) pointed out that these pronounced wind peaks are accompanied by development of baroclinically driven low-level jets. The speed of the sea breeze density current is estimated to be at about 2 m s^{-1}.

3.6. Half-hourly wind hodographs

The evolution of WS and WD on days controlled by sea breezes includes both theoretical and observational studies using hourly or half-hourly wind hodographs (Kusuda and Alpert, 1983; Steyn and Kallos, 1992). Analysis of wind hodographs is of great importance due to the role played by sea breeze dynamics in transporting photochemical pollutants (Lalas *et al.*, 1983). Friction, Coriolis and inertial forces were considered in a simplified linear model by Haurwitz (1947), which shows that elliptical hodographs always display clockwise rotation (CR) in the northern hemisphere. However, empirical studies (Zambakas, 1973; Prezerakos, 1986; Furberg *et al.*, 2002) have shown that local topography and profile of the coast (straight, convex or concave) induce pressure effects. These significant features can cause deviations from the theoretical sea breeze hodograph, resulting in an unexpected anticlockwise rotation (ACR). As Kusuda and Alpert (1983) concluded, ACR is not unusual and is possible in complex topography and coastline. Burk and Thompson (1996) computed hodographs at a height of ∼400 m avoiding local terrain effects.

Figure 12 displays the multi-year half-hourly wind hodographs for the 19 meteorological stations used (1) to

DOI: 10.1002/joc

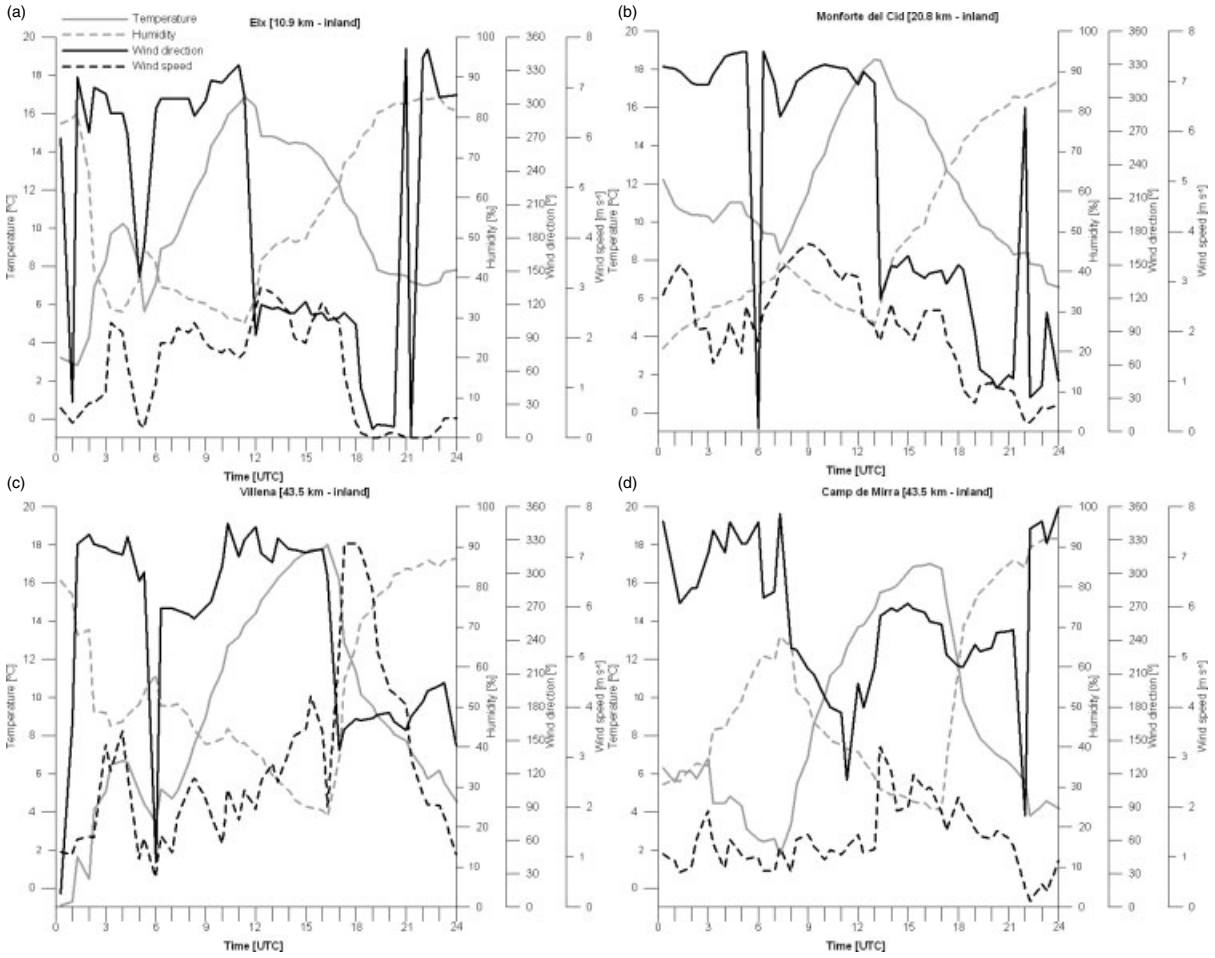

Figure 11. Daily evolution of TEMP, RH, WS and WD for a strong sea breeze front in (a) the Elx, (b) the Monforte del Cid, (c) the Villena and (d) the Campo de Mirra stations on 8 March 2008.

examine land–sea breeze rotation and (2) to devise statistical climatology (O_{time}; O_{ws}; O_{wd}; C_{time}; D_t; WS_{max}; WS_{time} and WD at the time of WS_{max}). The mean wind hodographs were calculated averaging the half-hourly wind vectors over the 475 sea breeze episodes selected. The number of sea breeze days used for each station is shown in Table I. The Agost, Camp de Mirra, Castalla, Catral, Crevillent, Elx, Monforte del Cid, Novelda, Orihuela, El Pinós, Planes and Villena hodographs show a marked ACR (Figure 12a), out of keeping with Haurwitz's (1947) linear model. The 12 ACR hodographs correspond to inland and prelittoral meteorological stations, where atmospheric circulation is strongly affected by the nearby Prebetic mountain ranges. The heated mountain slope causes thermally up-slope circulations and inland breezes, which can produce distortions of the observed multi-year hodographs (Kusuda and Alpert, 1983; Simpson, 1994). The dominance of the ACR ellipses is therefore mainly accounted for by the effect of local topography.

In contrast, Altea, Dénia, Ondara and Pilar de la Horadada coastal stations show a CR as expected CR due to the effect of Coriolis acceleration on the direction of wind rotation. The Almoradí hodograph, which is located 18 km from the nearest shoreline, also displays a CR (Figure 12b). No clear rotation was detected in the RS and La Vila Joiosa hodographs (Figure 12c). Table V presents the characteristics of sea breezes determined from the 19 wind hodographs for each station.

3.7. Effects of large-scale circulation

The synoptic environment is the most prominent factor controlling the degree of occurrence and persistence of sea breezes (Azorin-Molina and Martin-Vide, 2007). For instance, the long-lasting calm weather situations led to an increase in the occurrence of sea breeze days in the dry summer 2003 (52.0% in July and August). However, the study of the mean SLP field that allows mesoscale circulations to develop (e.g. lake and sea breezes) has not been given much consideration in the literature (Laird *et al*., 2001), and only few studies describe the main characteristics of sea breezes in relation to large-scale weather types (Damato *et al*., 2003). However, there are quite a number of studies that look at the occurrence of sea breezes as a function of the offshore component of the wind (Zhong and Takle, 1993), which also is a measure of the large-scale weather conditions. A detailed discussion about the influence of atmospheric conditions (e.g. synoptic scale flows) on the sea breeze

DOI: 10.1002/joc

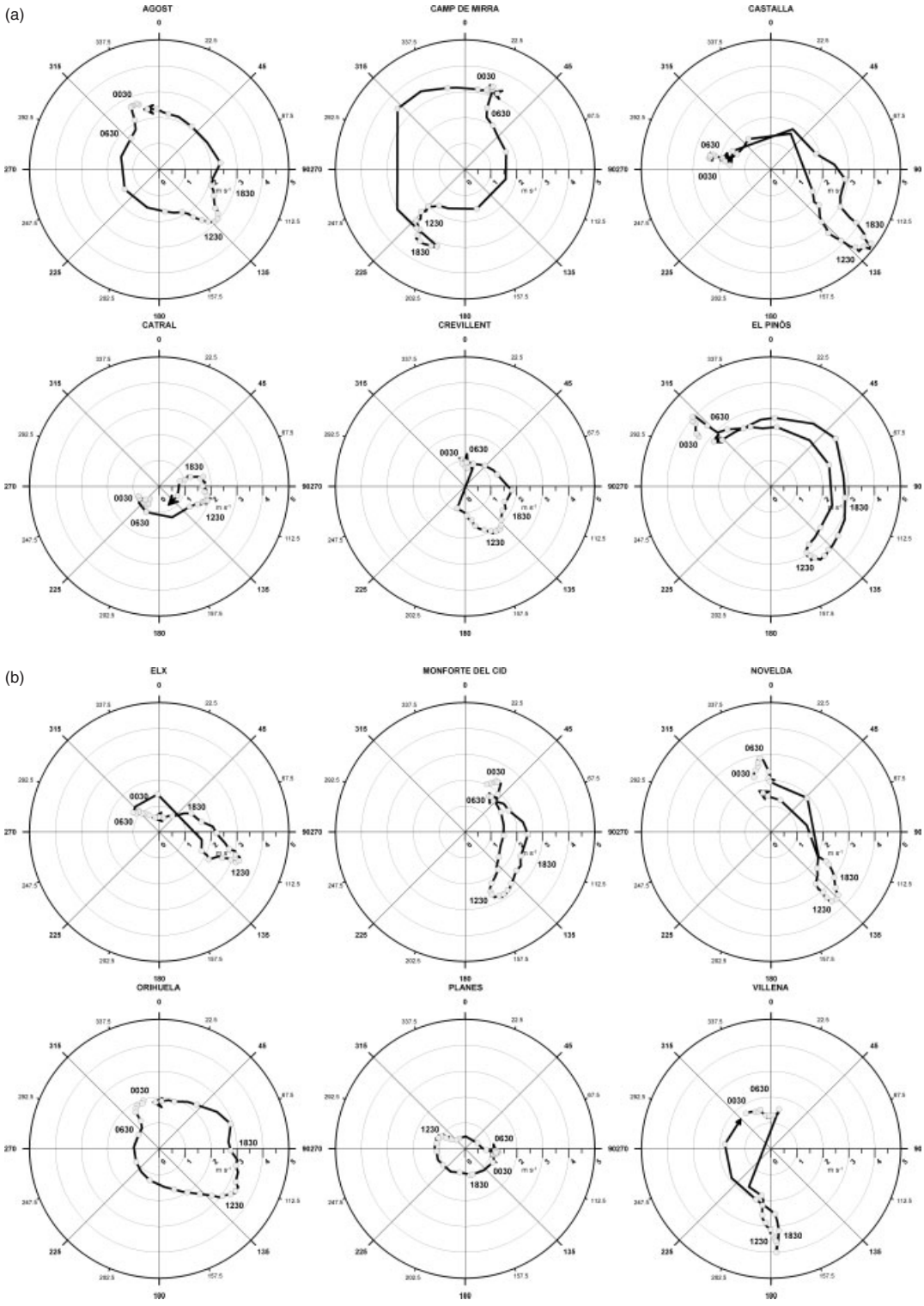

Figure 12. (a) Half-hourly wind hodographs averaged over the 475 pure sea breeze episodes at the RS during the 6-year study period (2000–2005) for the 12 inland and prelittoral stations listed in Table I. ACR hodographs. Units are in m s^{-1}. The numbers near the ellipse indicate the corresponding hour at UTC. (b) As in (a), except for the four coastal and one prelittoral (Almoradí) stations listed in Table I. CR hodographs. (c) As in (a), except for the two coastal stations listed in Table I. No clear rotation.

characteristics studied here can be found in Azorin-Molina and Chen (2009).

Figure 13 shows a comparison between the distribution of relative frequencies ($\sum n_i$, %) of Lamb's weather types (1) for the 475 sea breeze events and (2) for the 6-year period. Sea breezes were observed under all the 26 weather types in the Bay of Alicante, but only few of these circulation types are most important for the development of sea breezes. In general, the sea breezes in the Bay of Alicante tend to occur under the A weather type, which is the most frequent synoptic pattern (167 episodes, 35.2%). This frequency is higher than

DOI: 10.1002/joc

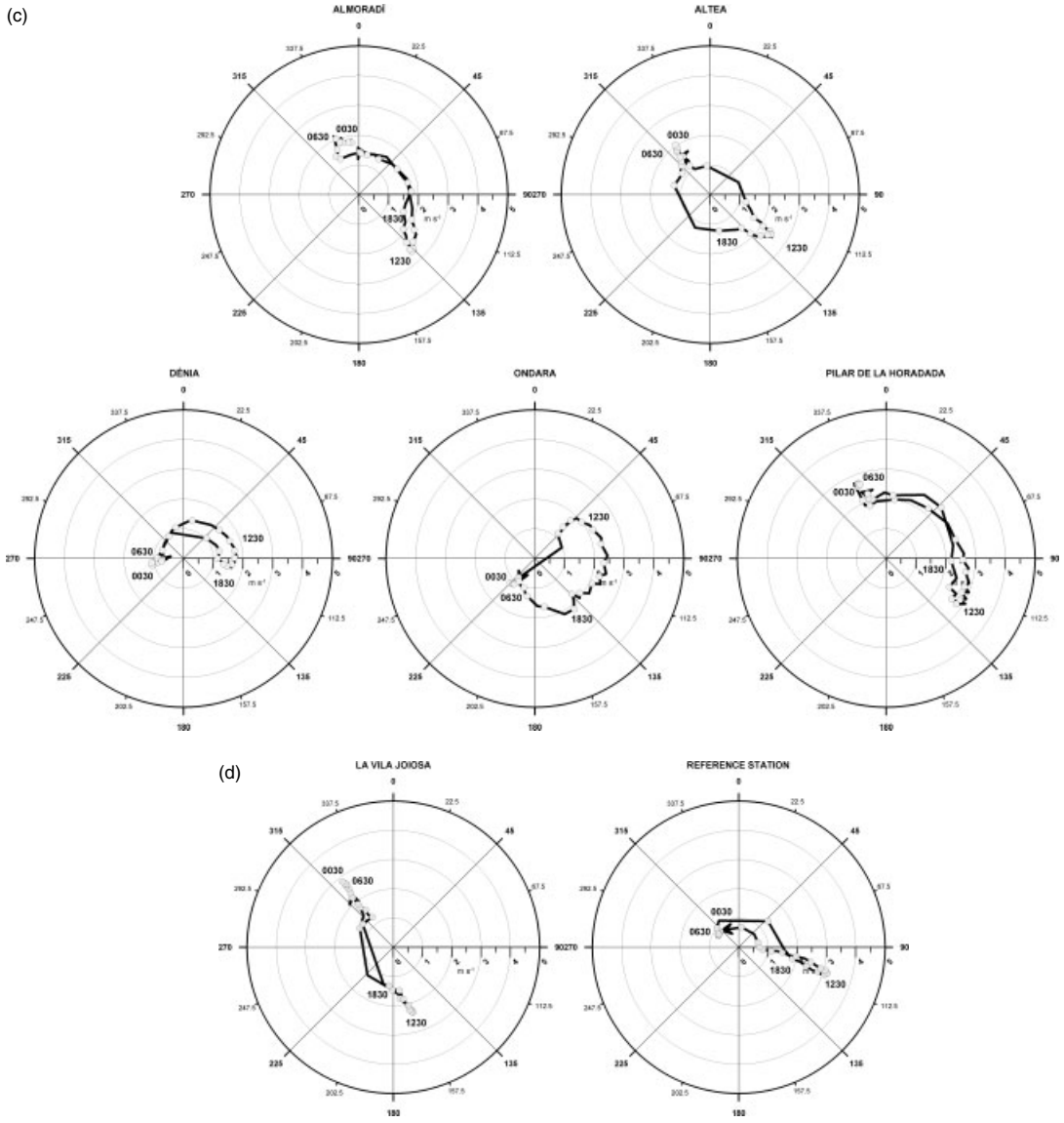

Figure 12. (*Continued*).

the A occurrence frequency for the whole study period (23.6%).

The next five most frequent synoptic patterns are C, N, NE, E and SE. However, the distribution of their relative frequencies is different during the sea breeze events and over the whole period. If we examine the 6 years, the distribution is as follows: C (10.0%), N (8.3%), NE (7.4%), E (7.2%) and SE (5.3%). During the sea breeze events the E (45 episodes, 9.5%) and NE (41 episodes, 8.6%) directional types are the second and third most frequent synoptic patterns, followed by the C (31 episodes, 6.5%), N (29 episodes, 6.1%) and SE (22 episodes, 4.6%) weather types.

The seventh and eighth most frequent synoptic systems for the whole study period correspond to the NW (4.7%) and W (3.9%) types, respectively. They are replaced by the AE (18 episodes, 3.8%) and the ANE (17 episodes, 3.6%) hybrid anticyclonic types for sea breeze events. These eight weather types account for 70.3% for the 6-year study period and 77.9% for the sea breeze events. The CSW (one episode, 0.2%), CNW and AS (two episodes, 0.4%), and CE, CS and ANW (three episodes, 0.6%) weather types are less favourable for sea breeze development.

Figure 14 shows the mean SLP fields during sea breeze events in the Bay of Alicante for the eight major weather types. The Azores high-pressure system dominates over the Eastern Atlantic and the IP (1024 hPa) in the composite SLP for the A type (Figure 14a), resulting in a weak surface pressure gradient, sunshine and fair weather (Ramis and Romero, 1995). This is the typical weather type for sea breeze development in winter.

The SLP for the E type (Figure 14b) presents an anticyclonic ridge surrounding Western Europe (1020–1024 hPa) and a low-pressure area over the north of Africa (1012 hPa), giving rise to a slightly easterly circulation over the western IP. However, a relatively weak surface pressure gradient covers the study area and sea breezes can develop.

DOI: 10.1002/joc

Table V. Basic characteristics of sea breezes determined from the 19 multi-year wind hodographs.

Station	O_{time} (UTC)	O_{wd} (°)	O_{ws} (m s^{-1})	C_{time} (UTC)	D_t (h)	WS_{max} (m s^{-1})	WS_{time} (UTC)	WD (°)
Agost	0830	172	1.64	2000	1130	2.96	1400	133
Almoradí	0930	76	1.68	2100	1130	2.67	1400	135
Altea	0900	111	1.50	1900	1000	2.52	1300	125
Camp de Mirra	0930	216	1.73	1900	0930	3.30	1600	210
Castalla	0830	118	1.82	2030	1200	4.89	1500	129
Catral	1000	116	1.58	2000	1000	2.03	1500	103
Crevillent	1000	167	1.50	2000	1000	2.19	1500	140
Dénia	1100	40	1.50	2030	0930	1.78	1400	87
Elx	0900	100	1.67	2000	1100	3.28	1430	110
La Vila Joiosa	0830	181	1.50	1900	1030	2.35	1300	164
Monforte del Cid	0830	126	1.62	2000	1130	2.89	1400	151
Novelda	0900	116	2.03	2000	1100	3.67	1500	136
Ondara	1000	43	1.63	2000	1000	2.45	1500	102
Orihuela	0900	172	1.50	2000	1100	3.41	1500	120
Pilar de la Horadada	0900	60	2.38	1930	1030	3.06	1500	120
El Pinós	0930	70	2.40	1930	1000	3.41	1500	146
Planes	0900	309	0.58	1900	1000	1.19	1300	290
Villena	1000	210	1.70	2230	1230	4.01	1930	177
RS	0900	94	1.59	2230	1330	3.17	1300	107

Last column (WD) corresponds to the WD at time of WS_{max}.
Times in this study are given in UTC: local time in Alicante is UTC +0100 h, or +0200 h with daylight-saving time.

A similar synoptic pattern, as shown for the E type, is displayed for the NE situation (Figure 14c), although the subtropical high pressure moves north of the Azores and a northeasterly circulation dominates. A weak pressure gradient also occurs over the province of Alicante. The mean SLPs for the hybrid anticyclonic AE (Figure 14d) and ANE (Figure 14e) types are similar to the E and NE types, respectively, with a ridge of high pressure oriented northeastward across the Eastern Atlantic.

The mean SLP field for the C type (Figure 14f) represents the typical SLP pattern that allows sea breeze to develop in summer (Ramis and Romero, 1995). A thermal low-pressure region in the vicinity of Africa surrounds the entire IP, leading to a weak pressure gradient throughout the area.

The composite SLP for the N type (Figure 14g) corresponds to high pressure over Azores, resulting in northerly circulation over the western IP. Eastern Spain and the Western Mediterranean basin are under the influence of a flat barometer.

Finally, the composite SLP for the SE type (Figure 14h) displays an anticyclonic blocking with a region of high pressure centred over the English Channel (1026 hPa) and a N–S low-pressure area from Morocco (1012 hPa) to Portugal. A southeasterly circulation results, but a weak anticyclonic ridge surrounds the province of Alicante and local wind circulations dominate.

4. Summary and concluding remarks

This paper presents the first attempt to study the climatology of sea breezes in the Bay of Alicante in Spain, using meteorological data from 6-year study period (2000–2005). On the basis of an objective selection technique for the reference station, 475 sea breeze episodes have been selected and the main parameters of the phenomenon have been determined, including: mean time of the sea breeze passage, mean wind speed and direction at the time of onset, mean time of sea breeze cessation, mean temporal dimension (duration), mean maximum velocity, mean time of maximum velocity and mean wind path of sea breezes. The major findings of this study can be summarized as follows:

1. The mean time of the onsets is 0940 UTC, and 0900 UTC is the most frequent onset time. The arrival of sea breezes fluctuates from ~0100–0200 h after sunrise in summer (0600 UTC) to ~0700–0800 h after sunrise in winter (1430 UTC). The earliest monthly mean onset time occurs at 0834 UTC in June (summer solstice) and the latest at 1241 UTC in December (winter solstice) strictly related to the physical factors characterizing the season (length of day, hours of sunshine, etc.) (Figure 3).
2. The mean half-hourly wind speed at the time of onset is 2.07 m s^{-1} and therefore wind at the passage of the sea breeze is generally light in the Bay of Alicante. April (2.19 m s^{-1}) and May (2.20 m s^{-1}) show a high mean half-hourly wind speed at the time of onset in relation to the biggest gradient of temperature between land and sea air, whereas November (1.82 m s^{-1}) presents the lowest mean value throughout the year (Figure 4).
3. At onset time, sea breezes tend to blow from 67.5°, 90° and 112.5°. A noteworthy monthly variation

DOI: 10.1002/joc

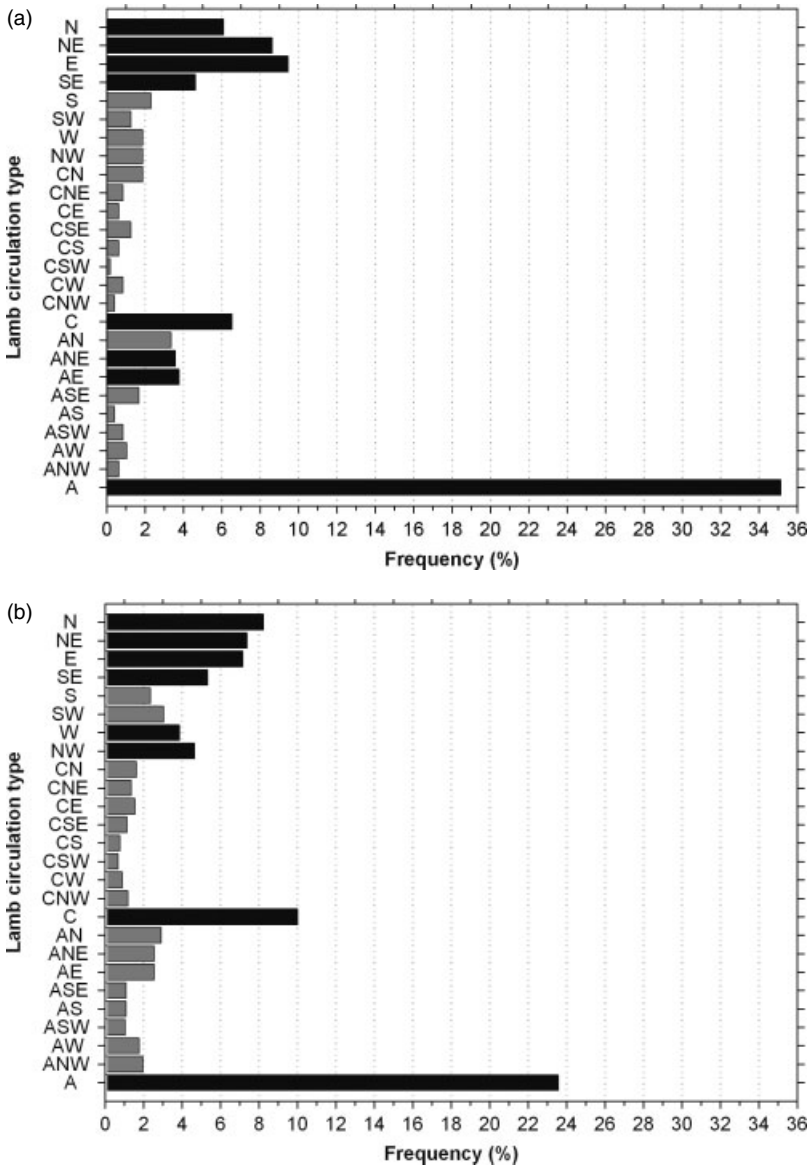

Figure 13. Histogram of the relative frequency distribution of the Lamb weather types (a) for the 475 sea breeze episodes and (b) for the 6-year study period (2000–2005).

is observed: sea breezes blow from 135° to 180° (southerly and southeasterly flows) during autumn and winter and from 67.5° to 112.5° (easterly winds) in the summer months. The daytime diabatic heating of the Prebetic mountain slope forces sea breezes to blow between 135° and 180° in winter (Figure 5).

4. Mean cessation time is 2009 UTC, with 2100 UTC being the most frequent class interval of time. The retreat of sea breezes varies from ∼1 h before sunset in winter (1630 UTC) to ∼0400–0500 h after sunset in summer (2330 UTC). The earliest mean monthly cessation time takes place at 1718 UTC in December (winter solstice) and the latest one occurs at 2128 UTC in July (a little after the summer solstice) (Figure 6).
5. Mean sea breeze duration is 1029 h, 1100 h being the most frequent class interval of time. The duration of sea breeze flows fluctuates from a minimum of 0230 h in autumn–winter to a maximum of 1600 h in summer. Mean monthly duration of the phenomenon gradually increases month-by-month from January (0459 h) to the highest mean in July (1248 h), whereas a steady decrease occurs from the central months of summer until December, when it reaches the lowest value (0437 h) (Figure 7).
6. The mean maximum velocity of sea breezes is 6.8 m s^{-1}, with a maximum of 11.6 m s^{-1} and a minimum of 3.6 m s^{-1}. Sea breezes are much more intense from April to August, particularly during spring, due to the biggest gradient of temperature between land and sea air. Weak sea breezes occur from September to March when the land–sea temperature gradient is smaller (Figure 8). The mean time of the maximum velocity of sea breezes is 1250 UTC, 1230 UTC being the most frequent class. The mean monthly time of maximum sea breeze velocity occurs earlier from April to August (1230 UTC in June) and later

DOI: 10.1002/joc

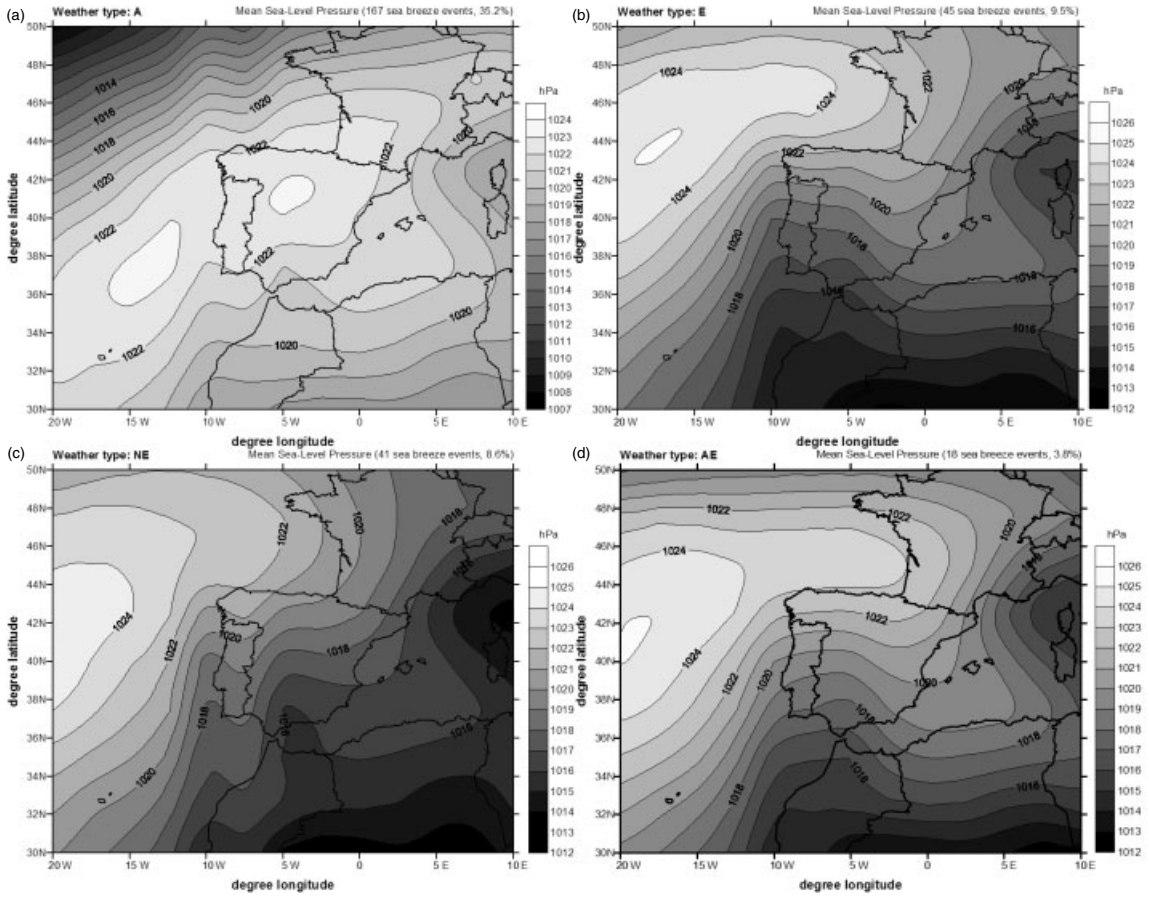

Figure 14. Mean sea level pressure (in hPa) field for the eight major circulation types averaged over the sea breeze events observed in the 6-year period: (a) A, (b) E, (c) NE, (d) AE, (e) ANE, (f) C, (g) N, (h) SE.

from September to March (1334 UTC in November) (Figure 9). In conclusion, the greater the differential heating between land and sea air during spring and summer months, the higher the maximum speed.

7. The mean wind path of sea breezes is 97.7 km, with a maximum of 224.7 km and a minimum of 18.4 km. Sea breeze wind paths generally penetrate between 25 and 175 km, with 100–125 km being the most frequent class. The highest mean monthly sea breeze wind path occurs in June (118.1 km), whereas the lowest inland directed wind path takes place in December (34.7 km) (Figure 10). A case study showed a deep propagation of sea breeze fronts with pronounced wind peaks inland in the late afternoon (Figure 11).

The analysis of the multi-year half-hourly wind hodographs shows that an unexpected anticlockwise rotation dominates in the inland and prelittoral stations because of the local topography, whereas a clockwise rotation, as expected in accordance with the Coriolis acceleration, is reported at the coastal stations. No clear rotation was detected in the reference station (Figure 12a, b, c). The JC weather-typing system shows that sea breeze develops mainly during eight large-scale circulation types: A, E, NE, AE, ANE, C, N and SE (Figures 13 and 14).

One of the future aims is to increase the number of comprehensive sea breeze data sets along the Iberian Mediterranean coast and in the Balearic Isles to create a denser network. The use of datasets for other locations would improve the statistics and comparisons of the main characteristics of sea breezes. There is also a need for in-depth study of other parameters of sea breezes over the region of Alicante, such as thickness, vertical (detection of the return current above sea breeze layers) and horizontal (wind fields on surface) structure, inland propagation considering the barrier effect of mountains, structure of sea breezes over sea, etc. In addition, this multi-year study is a good starting point for numerical simulations and observational techniques, which can serve to improve the results presented here.

Finally, these multi-year results constitute a very good basis for policy makers to determine the probability of sea breezes and their effect on the environment in a context of complex terrain and coastline. The high occurrence of sea breezes is the main factor controlling air pollution dynamics and problems of air quality in Mediterranean cities. The Bay of Alicante is subjected to great pressure from industry and road traffic. Consequently, sea breezes should be the subject of increasingly sophisticated research, due to the fact that they result in either improved or reduced air quality: transport,

DOI: 10.1002/joc

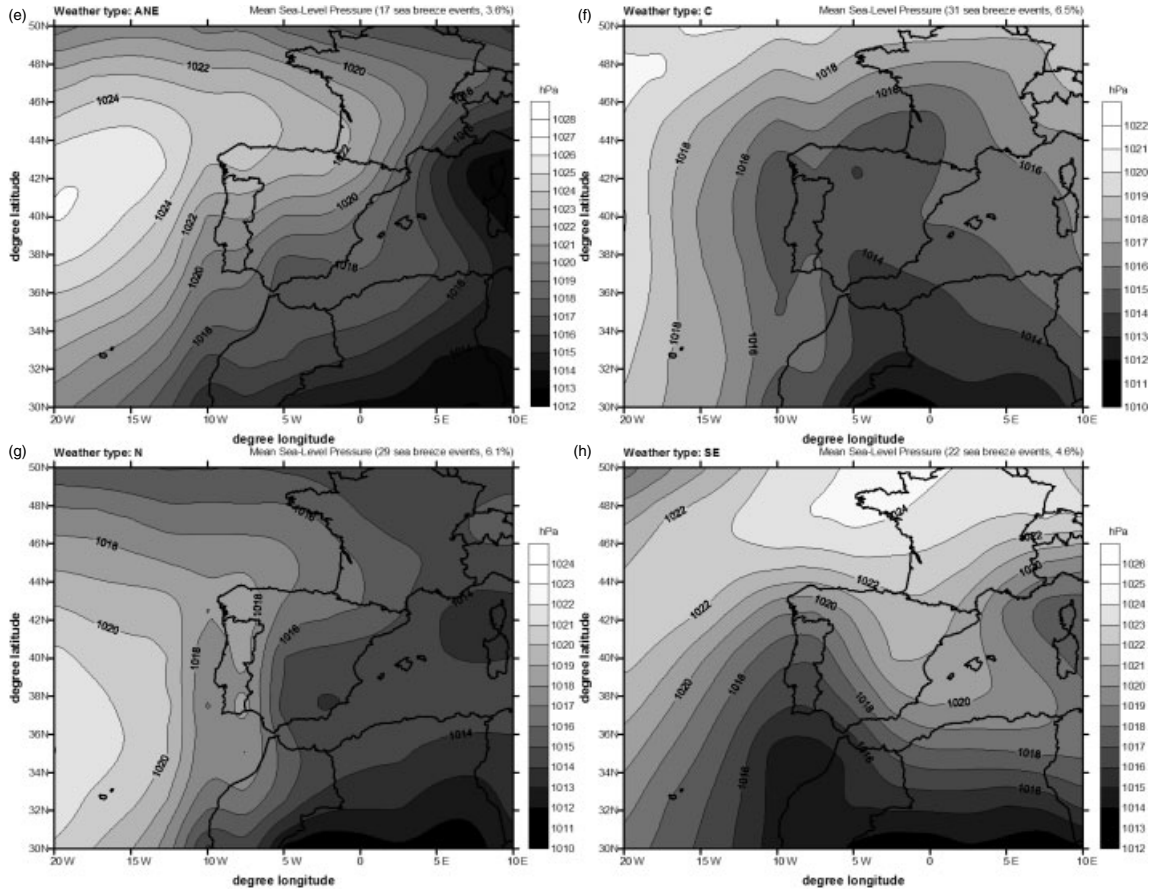

Figure 14. (*Continued*).

dispersion and concentrations of atmospheric aerosols. Air quality applications are a further step and represent the greatest motivation for continued study of sea breezes and local winds. Future sea breeze studies are of great scientific and environmental interest due to their impact on climate, air quality and human health, all of which calls for measures aimed at reducing air pollution.

Acknowledgements

The Fundacion CEAM is financed by the Generalitat Valenciana and BANCAIXA. This research has been undertaken in the frame of the CONSOLIDER-INGENIO 2010 Programme (GRACCIE project) and by the Torres Quevedo Program (PTQ-08-02-06762). The study was supported by Spain's Education and Science Ministry (MEC) project IPIBEX (CGL2005-07664-C02-01). The authors would like to thank the NCEP/NCAR Reanalysis project for providing sea level pressure data. Thanks are also due to the IVIA and the Institute of Coastal Ecology of El Campello that provided data. Contribution from M. Baldi was supported by the project: "Impatto del clima e della circolazione atmosferica locale sugli ecosistemi costieri mediterranei: la Tenuta Presidenziale di Castelporziano come caso di studio" funded by the Italian "Accademia delle Scienze detta dei XL".

References

Atkinson BW. 1981. *Meso-scale Atmospheric Circulations*. Academic press: London.

Azorin-Molina C. 2007. *A climatological study of sea breezes in Alicante. Sea-breeze fronts over the Iberian Mediterranean area and the isle of Mallorca*. PhD thesis. University Institute of Geography, University of Alicante, Alicante; 280.

Azorin-Molina C, Baldi M, Dalu G. 2008. An analytical study of the inland penetration of sea breezes in presence of complex topography. *Geophysical Research Abstract* **10**: EGU2008-A-05678.

Azorin-Molina C, Chen D. 2009. A climatological study of the influence of synoptic-scale flows on sea breeze evolution in the Bay of Alicante (Spain). *Theoretical and Applied Climatology* **96**: 249–260.

Azorin-Molina C, Martin-Vide J. 2007. Methodological approach to the study of the daily persistence of the sea breeze in Alicante (Spain). *Atmosfera* **20**: 57–80.

Borne K, Chen D, Nunez M. 1998. A method for finding sea breeze days under stable synoptic conditions and its application to the Swedish west coast. *International Journal of Climatology* **18**: 901–914, DOI: 10.1002/(SICI)1097-0088(19980630)18:8<901::AID-JOC295>3.0.CO;2-F.

Bowers LA. 2004. *The Effect of Sea Surface Temperature on Sea Breeze Dynamics Along the Coast of New Jersey*. Graduate School-New Brunswick Rutgers, The State University of New Jersey: New Brunswick, NJ.

Burk SD, Thompson WT. 1996. The summertime low-level jet and marine boundary layer structure along the California Coast. *Monthly Weather Review* **124**: 668–686, DOI: 10.1175/1520-0493(1996)124<0668:TSLLJA>2.0.CO;2.

Chen D. 2000. A monthly circulation climatology for Sweden and its application to a winter temperature case study. *International Journal of Climatology* **20**: 1067–1076, DOI: 10.1002/1097-0088(200008)20:10<1067::AID-JOC528>3.0.CO;2-Q.

Damato F, Planchon O, Dubreuil D. 2003. A remote sensing study of the inland penetration of sea breeze fronts from the English Channel. *Weather* **58**: 219–225, DOI: 10.1017/S1350482706002283.

Davenport AG. 1963. The relationship of wind structure to wind loading. In *Proceedings of the International Conference on Wind Effects on Buildings and Structures*, Teddington.

Dessouky TM, Jenkinson AF. 1975. *An Objective Daily Catalogue of Surface Pressure, Flow and Vorticity Indices for Egypt and its Use in Monthly Rainfall Forecasting*, *Synoptic Climatology Branch Memorandum, No. 46*. Meteorological Office: Bracknell.

Estoque MA. 1962. The sea breeze as function of the prevailing synoptic situation. *Journal of the Atmospheric Sciences* **19**: 244–250, DOI: 10.1175/1520-0469(1962)019<0244:TSBAAF>2.0.CO;2.

Frenzel CW. 1962. Diurnal wind variations in Central California. *Journal of Applied Meteorology* **1**: 405–412, DOI: 10.1175/1520-0450(1962)001<0405:DWVICC>2.0.CO;2.

Furberg M, Steyn DG, Baldi M. 2002. The climatology of sea breezes on Sardinia. *International Journal of Climatology* **22**: 917–932, DOI: 10.1002/joc.780.

Graybeal DY. 2006. Relationships among daily mean and maximum wind speeds, with application to data quality assurance. *International Journal of Climatology* **26**: 29–43, DOI: 10.1002/joc.1237.

Güsten H, Heinrich G, Cvitas T, Klasinc L, Rus B, Lalas DP, Petrakis M. 1988. Photochemical formation and transport of ozone in Athens, Greece. *Atmospheric Environment* **22**: 1855–1861.

Haurwitz B. 1947. Comments on the sea breeze circulation. *Journal of Meteorology* **4**: 1–8.

Jenkinson AF, Collison BP. 1977. *An Initial Climatology of Gales over the North Sea*, *Synoptic Climatology Branch Memorandum, No. 62*. Meteorological Office: Bracknell.

Johnson A Jr, O'Brien JJ. 1973. A study of an Oregon sea breeze event. *Journal of Applied Meteorology* **12**: 1267–1283, DOI: 10.1175/1520-0450(1973)012<1267:ASOAOS>2.0.CO;2.

Jones PD, Hulme M, Briffa KR. 1993. A comparison of Lamb circulation types with an objective classification scheme. *International Journal of Climatology* **13**: 655–663, DOI: 10.1002/joc.3370130606.

Justus CG, Mikhail A. 1976. Height variation of wind speed and wind distribution statistics. *Geophysical Research Letters* **3**: 261–264.

Kalnay E, Kanamitsu M, Kistler R, Collins W, Deaven D, Gandin L, Iredell M, Saha S, White G, Woollen J, Zhu Y, Leetmaa A, Reynolds R, Chelliah M, Ebisuzaki W, Higgins W, Janowiak J, Mo KC, Ropelewski C, Wang J, Jenne R, Joseph D. 1996. The NCEP/NCAR 40-year reanalysis project. *Bulletin of the American Meteorological Society* **77**: 437–471, DOI: 10.1175/1520-0477(1996)077<0437:TNYRP>2.0.CO;2.

Kitada T, Igarashi K, Owada M. 1986. Numerical analysis of air pollution in a combined field of land/sea breeze and mountain/valley wind. *Journal of Applied Meteorology* **25**: 767–784, DOI: 10.1175/1520-0450(1986)025<0767:NAOAPI>2.0.CO;2.

Kottmeier C, Palacio-Sese P, Kalthoff N, Corsmeier U, Fiedler F. 2000. Sea breezes and coastal jets in southeastern Spain. *International Journal of Climatology* **20**: 1791–1808, DOI: 10.1002/1097-0088.

Kusuda M, Alpert P. 1983. Anti-clockwise rotation of the wind hodograph. Part I: theoretical study. *Journal of the Atmospheric Sciences* **40**: 487–499, DOI: 10.1175/1520-0469(1983)040<0487:ACROTW>2.0.CO;2.

Laird NF, Kristovich DAR, Liang X-Z, Arritt RW, Labas K. 2001. Lake Michigan lake breezes: climatology, local forcing, and synoptic environment. *Journal of Applied Meteorology* **40**: 409–424, DOI: 10.1175/1520-0450(2001)040<0409:LMLBCL>2.0.CO;2.

Lalas DP, Asimakopoulos DN, Deligiorgi DG, Helmis CG. 1983. Sea breeze circulation and photochemical pollution in Athens, Greece. *Atmospheric Environment* **17**: 1621–1632.

Lamb HH. 1950. Types and spells of weather around the year in the British Isles. *Quarterly Journal of the Royal Meteorological Society* **76**: 393–438.

Linderson M. 2001. Objective classification of atmospheric circulation over southern Scandinavia. *International Journal of Climatology* **21**: 155–169, DOI: 10.1002/joc.604.

Lyons WA. 1972. The climatology and prediction of the Chicago lake breeze. *Journal of Applied Meteorology* **11**: 1259–1270, DOI: 10.1175/1520-0450(1972)011<1259:TCAPOT>2.0.CO;2.

Martin-Vide J. 2001. Limitations of an objective weather-typing system for the Iberian peninsula. *Weather* **56**: 248–250.

Miao J-F, Kroon LJM, Vilà-Guerau de Arellano J, Holtslag AAM. 2003. Impacts of topography and land degradation on the sea breeze over eastern Spain. *Meteorology and Atmospheric Physics* **84**: 157–170, DOI: 10.1007/s00703-002-0579-1.

Millán M. 2002. Ozone dynamics in the Mediterranean basin. A collection of scientific papers resulting from the MECAPIP, RECAPMA and SECAP projects. Air pollution Research Report No. 78. Centro de Estudios Ambientales del Mediterráneo (CEAM): Valencia.

Novak DR, Colle BA. 2006. Observations of multiple sea breeze boundaries during an unseasonably warm day in metropolitan New York City. *Bulletin of the American Meteorological Society* **87**: 169–174, DOI: 10.1175/BAMS-87-2-169.

Olcina-Cantos J, Azorin-Molina C. 2004. The meteorological importance of sea breezes in the Levant region of Spain. *Weather* **59**: 282–286, DOI: 10.1256/wea.176.03.

Ookouchi Y, Wakata Y. 1984. Numerical simulation for the topographical effect on the sea-land breeze in the Kyushu island. *Journal of the Meteorological Society of Japan* **62**: 864–879.

Physick WL. 1980. Numerical experiments on the inland penetration of the sea breeze. *Quarterly Journal of the Royal Meteorological Society* **106**: 735–746, DOI: 10.1002/qj.49710645007.

Prezerakos NG. 1986. Characteristics of the sea breeze in Attica, Greece. *Boundary-Layer Meteorology* **36**: 245–266, DOI: 10.1007/BF00118663.

Prtenjak MT, Grisogono B. 2007. Sea/land breeze climatological characteristics along the northern Croatian Adriatic coast. *Theoretical and Applied Climatology* **90**: 201–215, DOI: 10.1007/s00704-006-0286-9.

Ramis C, Jansá A, Alonso S. 1990. Sea breeze in Mallorca. A numerical study. *Meteorology and Atmospheric Physics* **42**: 249–258, DOI: 10.1007/BF01314828.

Ramis C, Romero R. 1995. A first numerical simulation of the development and structure of the sea breeze in the island of Mallorca. *Annales Geophysicae* **13**: 981–994.

Reed JW. 1974. Wind power climatology. *Weatherwise* **27**: 237–242.

Redaño A, Cruz J, Lorente J. 1991. Main features of the sea breeze in Barcelona. *Meteorology and Atmospheric Physics* **46**: 175–179, DOI: 10.1007/BF01027342.

Salvador R, Millán M. 2003. Análisis histórico de las brisas en Castellón. *Tethys* **2**: 37–51.

Segal M, Avissar R, McCumber MC, Pielke RA. 1988. Evaluation of vegetation effects on the generation and modification of mesoscale circulations. *Journal of the Atmospheric Sciences* **45**: 2268–2293, DOI: 10.1175/1520-0469(1988)045<2268:EOVEOT>2.0.CO;2.

Shair FH, Sasaki EJ, Carlan DE, Cass GR, Goodin WR, Edinger JG, Schacher GE. 1982. Transport and dispersion of airborne pollutants associated with the land breeze-sea breeze system. *Atmospheric Environment* **16**: 2043–2054.

Simpson JE. 1994. *Sea Breeze and Local Wind*. Cambridge University Press: Cambridge.

Smith ME (ed.). 1968. *Recommended Guide for the Prediction of the Dispersion of Airborne Effluents*. American Society of Mechanical Engineering: New York.

Spellman G. 2000. The application of an objective weather-typing system to the Iberian peninsula. *Weather* **55**: 375–385.

Steyn DG, Kallos G. 1992. A study of the dynamics of hodograph rotation in the sea breeze of Attica, Greece. *Boundary-Layer Meteorology* **58**: 215–228, DOI: 10.1007/BF02033825.

Stull RB. 1995. *Meteorology Today for Scientist and Engineers*. West Publishing Company: St. Paul, MN.

Vicente-Serrano SM. 2004. *Evolución espacio-temporal de las sequías en el sector central del valle del Ebro: causas y consecuencias ambientales*. PhD thesis. Department of Geography and Country Planning, University of Zaragoza.

Yan H, Anthes RA. 1987. The effect of latitude on the sea breeze. *Monthly Weather Review* **115**: 936–956, DOI: 10.1175/1520-0493(1987)115<0936:TEOLOT>2.0.CO;2.

Zambakas JD. 1973. The diurnal variability and duration of the sea breeze at the National Observatory of Athens, Greece. *Meteorological Magazine* **102**: 222–228.

Zhong S, Takle ES. 1993. The effects of large-scale winds on the sea-land-breeze circulations in an area of complex coastal heating. *Journal of Applied Meteorology* **32**: 1181–1195, DOI: 10.1175/1520-0450(1993)032<1181:TEOLSW>2.0.CO;2.